BULLETIN OF THE POLISH ACADEMY OF SCIENCES
TECHNICAL SCIENCES
Vol. 54, No. 4, 2006

A study on liquefaction susceptibility of some soils from the coast of Marmara sea

A. SAWICKI* and W. ŚWIDZIŃSKI

Institute of Hydro-Engineering, Polish Academy of Sciences, 7 Kościerska St., 80-328 Gdańsk-Oliwa, Poland

Abstract. The paper presents an estimation of liquefaction susceptibility of some soils from the coast of the Marmara Sea, which was heavily striken by the Kocaeli earthquake in 1999. Firstly, the results of field investigations are summarized. Then, the results of laboratory investigations of physical and mechanical properties of the soils collated from the sites investigated are presented. The mechanical properties relate to the compaction/liquefaction model of saturated soils. This model is briefly outlined, then respective experimental procedures dealing with its calibration described, and values of material parameters listed. Liquefaction potential of investigated soils is analysed using standard procedures, based on the grain size distribution curves and SPTs. Finally, the simulation of pore-pressure generation and onset of liquefaction of Turkish soils is carried out, using the compaction/liquefaction model. Discussion of some standard empirical procedures of estimation of liquefaction potential of saturated soils, conducted from the analytical point of view, is also presented.

Key words: liquefaction, Kocaeli earthquake, soil parameters, experimental investigations, analytical modelling.

1. Introduction

Soil mechanics is one of the most exciting specializations in technical sciences, as it deals with the matter, which cannot be classified easily using traditional criteria. Usually, students are taught that there are just three kinds of matter, namely gases, liquids and solids. Students of theoretical physics are more initiated as they know that there is the fourth kind of matter, designated as plasma. But almost nobody knows that there also exists the fifth kind of matter commonly known as sands, grains and other granular materials. Why is it so? Probably because water saturated granular materials display properties which are characteristic for both solids and liquids, depending on applied forces and some other factors. Such knowledge cannot be found in traditional soil mechanics textbooks.

Saturated soils consist of a solid skeleton with pores filled with water. A solid skeleton is built of mineral grains of varying shapes and sizes, and different surface properties. Such a granular structure may be loose or dense, depending upon the way in which the grains are packed together. Overall behaviour of such a mixture depends of the effective stresses in the soil skeleton. If they are compressive and do not exceed failure criteria, the soil skeleton is able to support additional loads and behaves macroscopically like a solid body. Under certain conditions such as, for example, cyclic or shock loadings, the pore water pressure may increase, reducing the effective stresses, and consequently reducing the shearing resistance of saturated soil. Under extreme conditions, the shearing strength may reach its residual value, as it behaves macroscopically as a liquid, which cannot support any load. Therefore, liquefaction is the process transforming saturated granular material from the macroscopically solid state to the macroscopically liquid state.

Research on soil liquefaction has been carried out for nearly forty years, and there exists substantial literature on the subject, including books such as, for example [1–4]. One can distinguish two main research directions, namely the empirical approach and theoretical modelling of the liquefaction related phenomena. Extensive discussion of various approaches to this interesting problem is presented in the state-of-the-art paper [5]. In the paper, the historical development of the subject is also presented, and some 160 key references quoted.

The results presented in the present paper deal with investigations of liquefaction susceptibility of some soils from the coast of the Marmara Sea, which was heavily striken by the Kocaeli earthquake on August 17. 1999. Ground failures and associated large deformations were significant features of this earthquake, including damage to coastal structures due to soil liquefaction, cf. [6–8]. The impact of the Kocaeli earthquake on the coastal area has been studied within the framework of UE research LIMAS programme (Liquefaction Around Marine Structures), which includes investigations of some soils from the region.

The aim of this paper is to present the results of these investigations, mainly from the point of view of liquefaction susceptibility of soils taken from selected sites, located on the coast of Izmit Bay, which is part of the Marmara Sea. The research programme included the field investigations, performed by the Turkish firm ZETAS, and laboratory investigations of soils collected from boreholes during the field campaign, which were performed in the laboratory of the Institute of Hydro-Engineering.

The field investigations included a total number of five boreholes accompanied by SPTs and five cone penetration CPTUs. The laboratory investigations included the determination of basic physical properties of soils, and their C/L (com-

*e-mail: as@ibwpan.gda.pl

paction/liquefaction) characteristics, which is the most original feature of the results presented.

The compaction/liquefaction characteristics are the following: compaction curves, compressibility and the cyclic shear stress-strain relations. These characteristics are the constitutive ingredients of the compaction/liquefaction (C/L) model proposed by Sawicki [9]. This model enables detailed studies of particular problems in which the cyclic loading induced pore-pressure accumulation and subsequent liquefaction take place, cf. [10,11].

After calibrating the C/L model for the Turkish conditions, it was applied to simulate the pore-pressure generation and subsequent liquefaction for various cyclic shear stress histories. Extensive discussion of liquefaction susceptibility of investigated soils is also presented.

The importance of the present paper is that we show the results of very complex investigations of liquefaction susceptibility of saturated granular soils, which include the field and laboratory studies, application of empirical methods and theoretical modelling. Such a complex approach to the problem of liquefaction is original, as there exists a large gap between theoretical and practical soil mechanics. The aim of the present paper is also to make this gap narrower, and to test the prediction potential of the C/L theoretical model, elaborated in the Institute of Hydro-Engineering some years ago.

2. Sites investigated

Extensive information about various aspects of the Kocaeli Earthquake have already been published in a special issue of "Earthquake Spectra" [6]. The damage caused by this earthquake to marine and coastal structures was described in such other publications as, for example [7,8]. Therefore, in this paper only certain basic information will be summarized.

The Kocaeli Earthquake was one of the most destructive earthquakes ever to strike Turkey. Its magnitude was estimated as $M_w = 7.4$, and duration was 42 s. According to the official data, some 18000 people were killed and 44000 injured. More than 500000 people were left homeless. 115000 buildings collapsed or were damaged beyond repair, and the structural damage was estimated as high as 40 billion USD. Non-structural damage adds greatly to this huge loss.

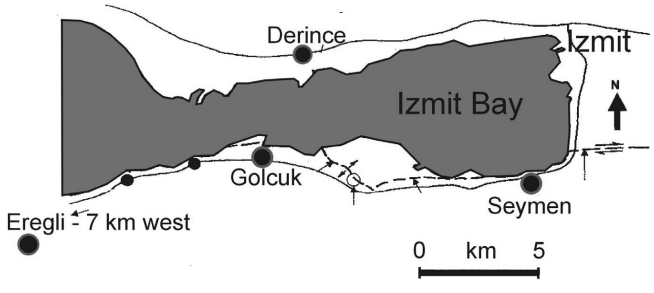

Fig. 1. Location of selected sites

Amongst many of the earthquake-induced phenomena, liquefaction-related problems played a significant role, including the coastal zone of Marmara Sea. The investigations have been limited to the following four sites located around the Izmit Bay: Port of Derince, Seymen, Kavakli-Gölcük and Eregli Fishery Harbour, see Fig. 1. A brief characteristic of these sites with respect to the damage caused by liquefaction related phenomena is presented below.

Derince Port. The total length of the waterfront structures in the Port of Derince is about 1.5 km. The earthquake caused damage to some quay-walls, which were displaced seawards even up to 0.7 m. Large settlements of backfill occurred, even down to 0.8 m, and sand boils were observed, which were signs of liquefaction. Also a large reclamation area settled below the water level, presumably due to liquefaction. Some cranes on rails tilted, and one crane was overturned.

2.1. Seymen. Several apartment blocks of 6 to 7 storeys, located some 40 to 50 m to the shoreline, suffered from liquefaction, and some collapsed totally. Liquefaction-induced damage was also characterised by large settlements of these blocks (partial sinking), approaching 2 m.

Kavakli-Gölcük. Large soil movements and subsidence occurred, probably triggered by soil liquefaction. As a result of these movements, a large part of coastal area was flooded. Sand boils were observed in many places, as well as large settlements of backfill (of the order of 1 m).

Ereğli Fishery Harbour. Seaward displacements of quay-walls and backfill settlements were observed. The breakwater settled approximately 1.5 m.

3. Geotechnical characteristics of chosen sites

Field investigations, performed by the Turkish firm ZETAŞ, included a total number of five boreholes accompanied by SPTs and five cone penetration CPTUs up to the depth of 20 m each. SPTs were performed with regular intervals of 1.5 m, according to ASTM D-1586 standard. They served mostly for determination of in-situ relative density of non-cohesive soils. The cone penetration tests, with pore water pressure measurement, have provided additional information regarding the in-situ shear strength of soils investigated and their compressibility characteristics. CPTUs were carried out using van den Berg equipment.

In the Port of Derince two boreholes were made. The first (BH-4) was located in the backfill area, 50 m from the seawall of berth No 5. The second (BH-5), 270 m from this berth. A single borehole (BH-1) in Seymen was made near the block which significantly settled due to liquefaction. Also single boreholes were made in the other locations: BH-2 in Kavakli-Gölcük near the land scrap, and BH-3 in the backfill of the Ereğli Fishery Harbour, close to the part of breakwater which settled significantly. Respective borehole logs with SPT diagrams are shown in Fig. 2.

The borings were performed using conventional rotary drilling method. The soil samples were taken, in the disturbed form, from depths corresponding to SPTs, in order to determi-

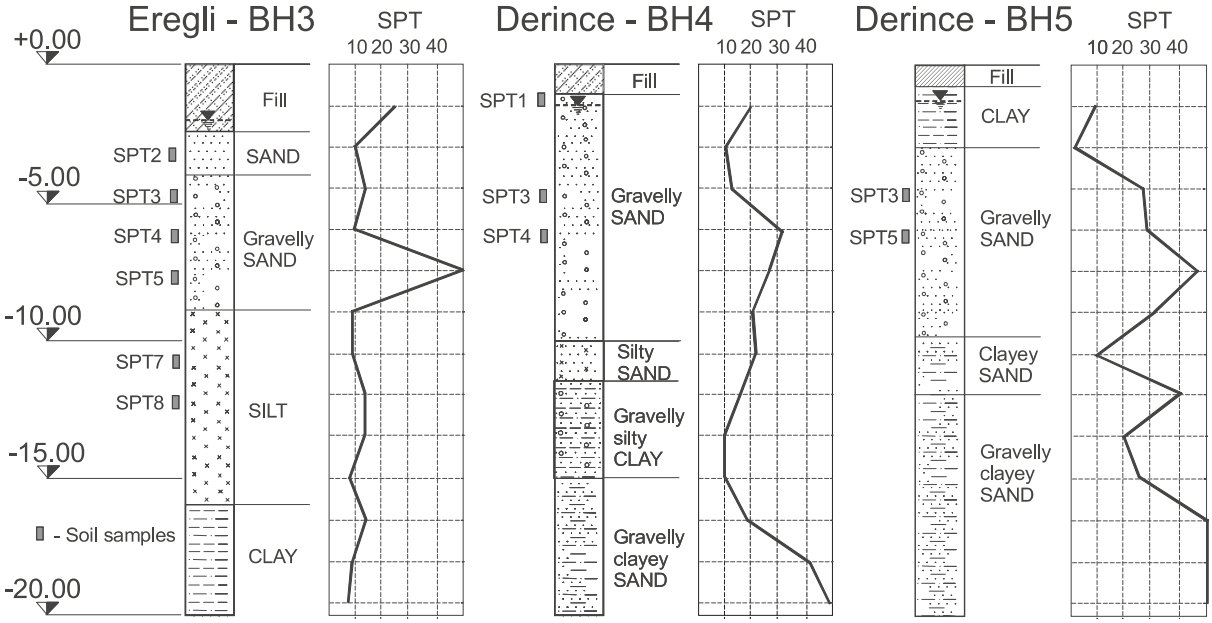

Fig. 2. Borehole logs of chosen sites, after ZETAŞ

Table 1
Physical properties of chosen soils

Borehole	No. of sample	Run [m] b.s.l.	Soil*	G_s	$e_{\min}$	$e_{\max}$	d_{10} (mm)	d_{60} (mm)	C_U	W [%]
BH1	SPT 2	1.50÷1.95	MS	2.55	0.81	1.54				44.5
	SPT 4	6.00÷6.45		2.77						62.6
BH2	SPT 2	3.00÷3.45	G-M (S-M)**	2.85	0.30	0.71	0.038	1.75	46.1	7.00
	SPT 5	7.50÷7.95	SM	2.78	0.64	1.44	0.006	0.135	22.5	22.6
	SPT 2	3.00÷3.45	S-M	2.68	0.61	1.21	0.04	0.11	2.75	24.0
	SPT 3	4.50÷4.95	G-M (S-M)**	2.69	0.39	0.84	0.02	0.40	19.8	12.9
BH3	SPT 4	6.00÷6.45	S-M	2.66	0.56	1.06	0.08	0.18	2.25	20.6
	SPT 5	7.50÷7.95	SM	2.71	0.63	1.49	0.003	0.096	32.0	23.1
	SPT 7	10.50÷10.95	M	2.73	0.93	1.99		0.04	>40	29.1
	SPT 1	1.00÷1.50	S-M+G	2.73	0.36	0.88	0.047	0.62	13.2	14.1
BH4	SPT 3	4.50÷4.95	SW+G	2.72	0.44	0.90	0.076	0.58	7.6	16.0
	SPT 4	6.00÷6.45	S-M+G	2.73	0.29	0.77	0.047	1.15	24.5	9.90
BH5	SPT 3	4.50÷4.95	S-M+G	2.69	0.30	0.79	0.05	0.8	16.0	12.8
	SPT 5	7.50÷7.95	S-M	2.69	0.37	0.94	0.064	0.32	5.0	15.2

* – according to BS 5930
** – after removal of over 6.3 mm cobbles

ne the main parameters. The first group of parameters characterizes the basic physical and strength properties such as natural moisture content, specific gravity, particle size distribution curves, the maximum and minimum void ratios, permeability coefficients, coefficients of earth pressures at rest, the angles of internal friction and cohesion. These parameters were determined using standard geotechnical methods. The strength parameters were also investigated in direct shear and triaxial apparatus. Table 1 collates the values of the above mentioned parameters.

Special attention was paid to silts which are significant components of the near surface soil deposits. In order to determine their physical and model parameters, they were first well dried and crushed to a very fine structure, and then tested as dry non-cohesive soil.

4. Empirical assessment of liquefaction potential

Extensive empirical research carried out for almost forty years, following disastrous earthquakes in Alaska and in Niigata, has led to elaboration of practical guidelines enabling assessment of liquefaction potential of soils. Recent publications of [12] or [13] summarize these achievements, see also [14].

The procedure suggested in [13] consists of two steps. During the first step, the grain size distribution curves and results of SPTs are analysed. If the results of this analysis are close to the borderline dividing the regions of liquefaction and non-liquefaction conditions, then the second step i.e. cyclic triaxial tests, should be performed. Other approaches, based on CPTUs, the Seismocone, etc., are also recommended in the above cited publications.

4.1. Analysis of the grain size distribution curves. Figures 3 and 4 show the grain size distribution curves collected from the boreholes BH3, BH4 and BH5, where the first number of respective curve corresponds to the number of the borehole, whereas the second number represents the number of sample taken from this borehole, (see Table 1). These curves should be compared with the limits defining the zones of high possibility of liquefaction and just a possibility of liquefaction, as recommended in [13], after official Japanese guidelines. The curves bounding the regions of high possibility of liquefaction and just a possibility of liquefaction have been designated as Tsuchida's curves, cf. [14].

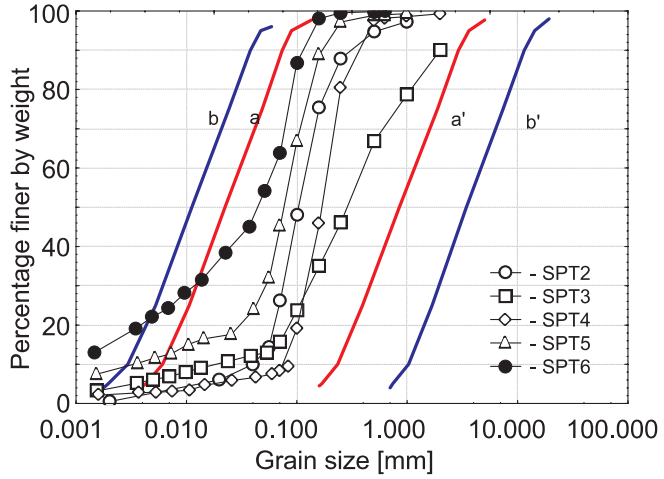

Fig. 3. Grain size distribution curves of soils from Eregli Fishery Port against Tsuchida's curves. Region bounded by curves a and a': zone of high possibility of liquefaction. Zone of possibility of liquefaction is between curves b and b'

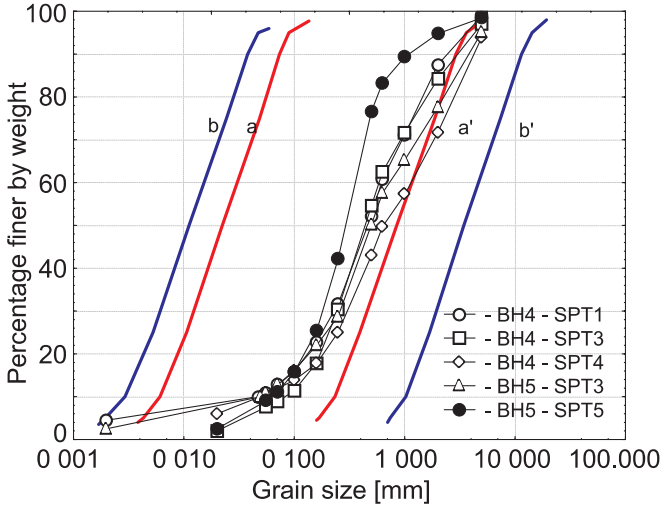

Fig. 4. Grain size distribution curves of soils from Derince Port against Tsuchida's curves

Consider, for example, the curves corresponding to the backfill in the Port of Derince, collected from different depths of BH4 and BH5. The largest parts of these curves are located within the zone of high possibility of liquefaction, but the upper parts of these curves are in the region of possible liquefaction. The PIANC guidelines suggest that, in this case, the second step of analysis should be performed, as the grain size distribution curves are close to the bounding curves. However, the PIANC recommendations are very general, as they do not specify precisely the liquefaction criteria. Interpretation of the grain size distribution curves is also not precise. The Derince soils contain not so much fines, so from this point of view these soils are susceptible to liquefaction. On the other hand, they contain too much gravel, which is very permeable and therefore prevents liquefaction. Interpretation of these results is difficult, as it is strongly dependent on subjective judgement. Anyway, a general conclusion is that the Derince soils have the possibility to liquefy.

In the case of Eregli soils (Fig. 3), the conclusions are similar, and the difference is that these soils contain more fines than those from Derince. It should be noted, that the above analysis is very rough, as it is based on only a single characteristic, which is the grain size distribution curve. An another important information is missing, namely the initial relative density of a given soil. Recall, that particular soils, characterised by the same grain size distribution curves, may also be characterized by different packing (dense or loose), not to mention the fabric. These factors have not been taken into account in the first step of empirical analysis of liquefaction properties of granular soils.

However, PIANC recommends a supplementary analysis of SPTs, which have been designed mainly to estimate the relative density of natural soil deposits. The relative density of granular soil is the other main factor, which informs about their liquefaction properties. Loose soils liquefy more easily than dense ones. Therefore, we have to supplement the grain size distribution curves analysis, with the other examination dealing with interpretation of SPTs results.

4.2. Interpretation of SPTs. Figure 5 shows the empirical interpretation of SPTs for soils from Eregli and Derince, elaborated according to standard geotechnical procedures, cf. Section 9. On the vertical axis, there is the cyclic stress ratio (CSR) defined as τ_{av}/σ'_v, where τ_{av} = estimated earthquake-induced shear stress; σ'_v = initial overburden vertical effective stress, see Eq. (19). On the horizontal axis there is the corrected blow count $(N_1)_{60}$, calculated from the following formula:

$$(N_1)_{60} = N_m C_N C_E C_B C_R C_S, \tag{1}$$

where: N_m = measured standard penetration resistance (see Fig. 2); C_N (see Eq. 2) = factor normalizing the measured blow counts to an effective overburden stress 100 kPa; $C_E = 1$ = correction for hammer energy; $C_B = 1$ = correction factor for borehole diameter; C_R = correction factor for the rod length (calculated according to [12], see also Table 2); C_S = correction for a standard sampling method = 1.

According to [15]:

$$C_N = \left(\frac{100}{\sigma'_{v0}}\right)^{0.5}, \tag{2}$$

where σ'_{v0} is an effective overburden pressure in kPa. C_N cannot be greater than 1.7.

The respective empirical data, corresponding to the Eregli and Derince soils, are shown in Fig. 5, together with the liquefaction resistance curves (CRR), corresponding to various fines contents, i.e. 5%, 15% and 35% or less. At each empirical point, a corresponding value of fines content is shown. The boundary curves correspond to the maximum horizontal acceleration of ground surface of 0.25 g, which is roughly similar to that recorded in analysed sites.

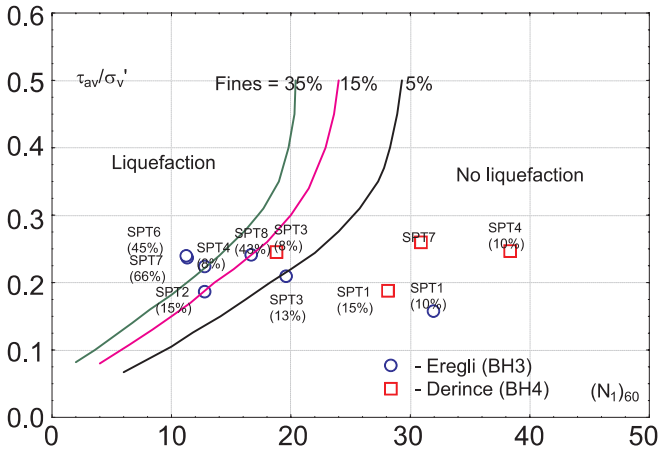

Fig. 5. Empirical interpretation of SPTs for soils from Eregli and Derince

The results obtained are quite different from those obtained from the analysis of the grain size distribution curves. For example, most of the points corresponding to the Derince backfill are located in the non-liquefiable region, contrary to the previous analysis. The points corresponding to the Eregli soils are located non-uniquely. For example, consider circles in Fig. 5 corresponding to Eregli soils, denoted as SPT3 and SPT4. Both points correspond to gravely sand, collated from the same layer (see Fig. 2). The fines contents do not differ greatly (8% v. 13%), neither blow counts (14 v. 10). But according to the standard interpretation of SPTs, liquefaction at point SPT4 is very likely, while the soil at point SPT3 is non-liquefiable.

The above discussion shows that the SPTs results do not precisely inform about liquefaction properties of investigated soils. Recall, that it follows from the post-earthquake inspections, that both the Derince and Eregli soils had liquefied.

5. Compaction/liquefaction model

The second group of parameters is strictly related to the compaction/liquefaction model, which has already been presented in other publications, cf. [9,16]. However, for the sake of self-consistency of this paper, a mathematical structure of the compaction/liquefaction model will be briefly outlined in this Section.

The behaviour of dry sand (or fully saturated, but with free drainage of pore water allowed) is described by two constitutive equations. The first describes the compaction due to cyclic shearing, and is formulated in the following differential form:

$$\frac{d\Phi}{dN} = D_1 J \exp(-D_2 \Phi), \tag{3}$$

where Φ denotes compaction, defined as irreversible porosity change:

$$\Phi = \frac{n_0 - n}{n_0}. \tag{4}$$

The other symbols are defined as follows: n_0 = initial porosity; n = current porosity; N = number of loading cycles treated as a continuous variable; D_1 and D_2 = material parameters characterizing densification properties, and J = the second invariant of the deviator of cyclic strains amplitudes tensor $\hat{E}^{dev}$:

$$J = \frac{1}{2} tr(\hat{E}^{dev})^2. \tag{5}$$

The second constitutive equation describes the dependence between the deviators of cyclic stress and strain amplitude tensors:

$$\hat{T}^{dev} = 2G\hat{E}^{dev}, \tag{6}$$

where $\hat{T}^{dev}$ = deviator of the tensor of cyclic stress amplitudes; G = shear modulus which depends on the mean effective stress.

In the case of saturated sand in undrained conditions, the following equation relates potential compaction to the pore pressure accumulation:

$$\frac{du}{dN} = \frac{1}{a}\frac{d\Phi}{dN}, \tag{7}$$

where u is an excess pore pressure generated by cyclic loadings; and

$$a = \frac{1 - n_0}{n_0}\kappa_s. \tag{8}$$

The parameter κ_s has a meaning of elastic compressibility of the soil skeleton.

There are four parameters defining the model, namely D_1, D_2, G and a, which should be determined experimentally.

6. Compaction properties

In this Section, a method of determination of the parameters D_1, D_2 appearing in Eq. (3) will be described, and values of these parameters for the Turkish soils presented. The above parameters were determined from experiments performed in the cyclic simple shear apparatus, specially constructed in the Institute of Hydro-Engineering, see Fig. 6. The basic idea of this apparatus is shown in Fig. 7.

The sample of soil, characterized by a given initial relative density D_r, is placed in the rectangular box with sides moving in one plane, in such a way that the sinusoidal cyclic shear strain at constant amplitude γ_0 takes place. The volumetric strain $\varepsilon_V = \Delta h/h_0$, where h_0 = initial height of the sample, is recorded as a function of the number of loading cycles N. Several experiments, performed at different shear strain amplitudes γ_0, lead to the determination of compaction curves, which illustrate the mean volumetric changes of sand due to cyclic loading, see Fig. 7. The results of experiments can be

presented by a common compaction curve in a new co-ordinate system z, Φ defined as follows:

$$\Phi = \frac{1-n_0}{n_0}\varepsilon_v, \tag{9}$$

$$z = \frac{1}{4}\gamma_0^2 N. \tag{10}$$

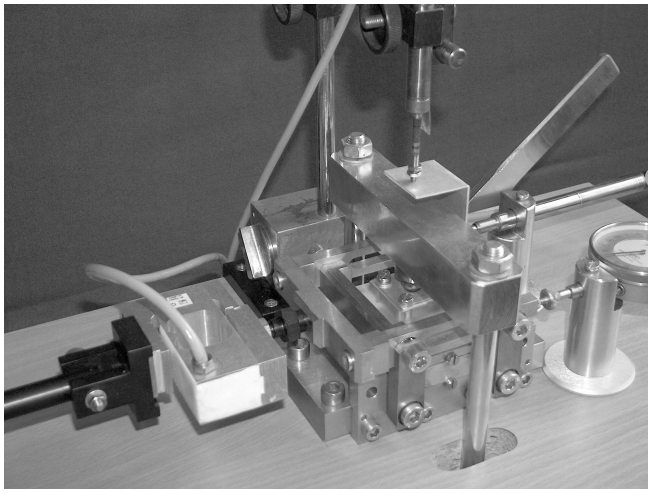

Fig. 6. Cyclic simple shear apparatus

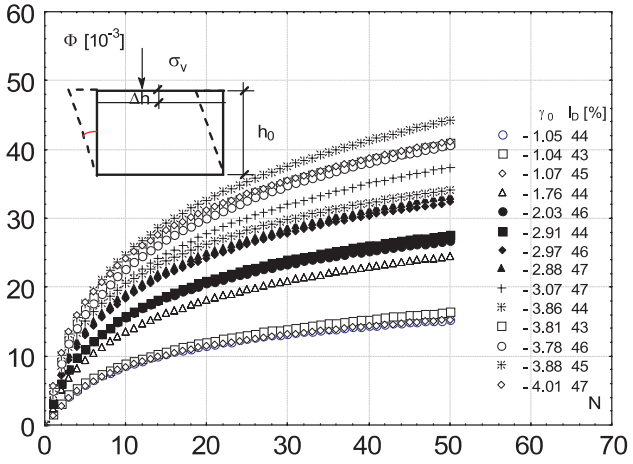

Fig. 7. Basic idea of cyclic simple shear apparatus and compaction curves; compaction curves correspond to Derince gravelly sand (BH5-SPT3)

Figure 8 shows the common compaction curve for the data from Fig. 7, which correspond to the Derince gravelly sand, characterized by the average, initial relative density $D_r = 0.45$, similar to the measured density of the soil deposit in the borehole BH5. This common compaction curve can be approximated by the following relation:

$$\Phi = C_1 \ln(1 + C_2 z), \tag{11}$$

where $C_1 = 9.57$ and $C_2 = 0.35$ in this special case. The parameters D_1 and D_2 can be calculated from the following formulae:

$$D_1 = C_1 C_2, \quad D_2 = \frac{1}{C_1}. \tag{12}$$

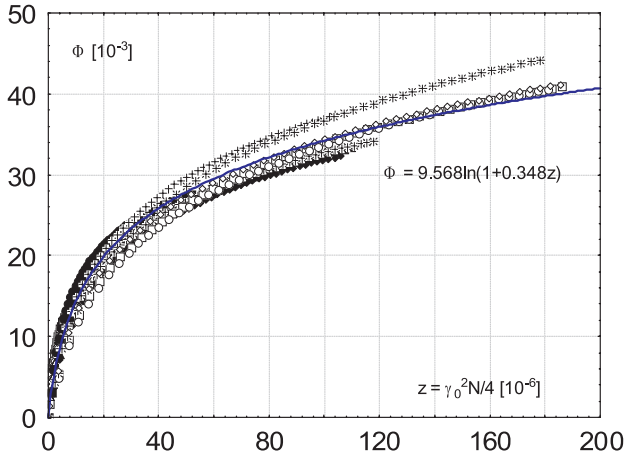

Fig. 8. Common compaction curve for data from Fig. 7

Table 2 shows the compaction coefficients D_1 and D_2 determined for soils taken from the boreholes shown in Fig. 2. These numbers correspond to the strain unit 10^{-3}. For example if $\gamma_0 = 2 \times 10^{-3}$, and $N = 8$, we calculate z (Eq. 10) as follows $z = \frac{1}{4} \times 2^2 \times 8 = 8$. Then we substitute this value into Eq. (11) in order to calculate the compaction: $\Phi = 9.57 \ln(1 + 0.35 \times 8) = 12.78$, which means that actual compaction is 12.78×10^{-3}.

7. Cyclic shear stress-strain relation

A general form of the relationship between cyclic shear stress and strain amplitudes is given by Eq. (6), where $G = G(p')$ plays the role of shear modulus, and p' is the mean effective stress. In the case of triaxial compression, Eq. (6) takes the following simple form:

$$(\sigma_1 - \sigma_3) = 2G\,(\varepsilon_1 - \varepsilon_3)\,, \tag{13}$$

where σ_1 = vertical cyclic stress, σ_3 = horizontal cyclic stress, ε_1 = vertical cyclic strain and ε_3 = horizontal cyclic strain.

During a single experiment, the sample was first anisotropically pre-consolidated to a certain stress level characterised by $p = p^*$ and $q = q^*$, where:

$$p = \frac{1}{3}\,(\sigma_1 + 2\sigma_3)\,, \tag{14}$$

$$q = \sigma_1 - \sigma_3. \tag{15}$$

The values of $p*$ and $q*$ are marked in Fig. 9. They correspond to the mean values of the mean and deviatoric stresses, around which the cyclic loading takes place.

After anisotropic pre-consolidation, the pressure in the cell was kept constant (σ_3 = const) and the vertical stress was cyclically changed. Respective stress paths in the p, q space are shown in Fig. 9.

Each stress path corresponds to a different experiment, characterised by different mean stresses p^* and q^*, as the dependence of the shear modulus on the initial stress should be found. A typical record of the stress-strain relation is shown in Fig. 10. In the compaction/liquefaction model we neglect the shear hysteresis, and only the mean slope of the stress-strain

curves is of interest to us, excluding the first cycle, as we are interested in the cyclic shear stress-strain response. The cyclic loading shear modulus G was determined from the mean slope of the stress-strain curves, using Eq. (13).

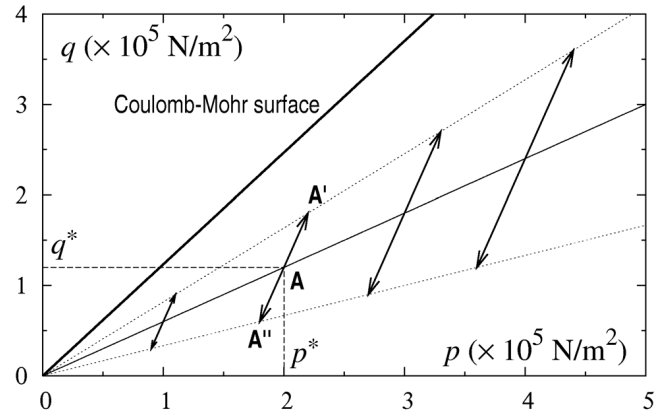

Fig. 9. Cyclic loading stress paths in the triaxial apparatus for determination of cyclic loading shear modulus

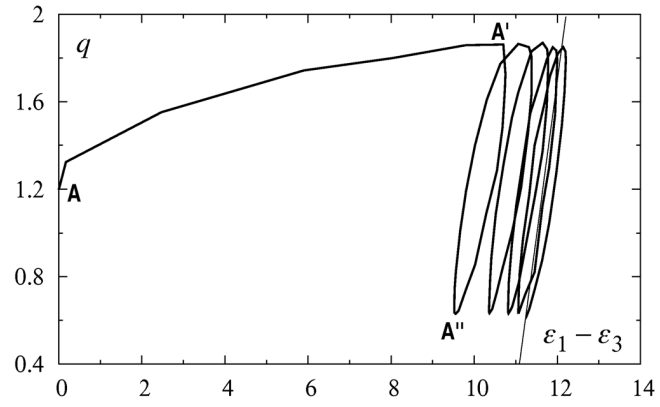

Fig. 10. Typical cyclic stress-strain relation

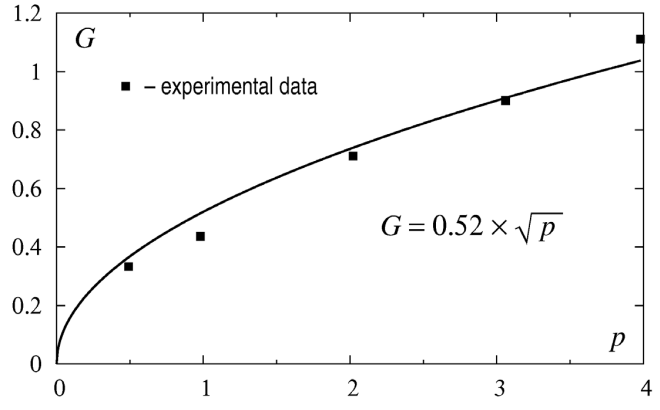

Fig. 11. Dependence of the cyclic shear modulus on the mean stress for Ereğli sand

Figure 11 shows the relationship between the cyclic shear modulus and average mean stress determined for the Ereğli sand (borehole BH-3, SPT4 – at depth of 6 m). The following formula, which is already well known in soil mechanics, approximates the experimental results:

$$G = 0.52\sqrt{p'} = G_1\sqrt{p'}. \tag{16}$$

Here, p' should be substituted in stress unit 10^5 N/m^2, and G is obtained in modulus unit 10^8 N/m^2. For example, for $p' = 1 \times 10^5$ N/m^2, we substitute into Eq. (16) $p' = 1$, and obtain $G = 0.52$, which means that the true value of this modulus is 0.52×10^8 N/m^2. The values of G_1 for other soils are shown in Table 3.

8. Skeleton's compressibility

The elastic compressibility of the soil skeleton was determined from the experiments performed in a specially constructed oedometer which enables measurement of lateral stresses. The idea of the measurement and the method of determination of elastic moduli is described in [17,18]. This method is based on the analysis of the soil behaviour during unloading.

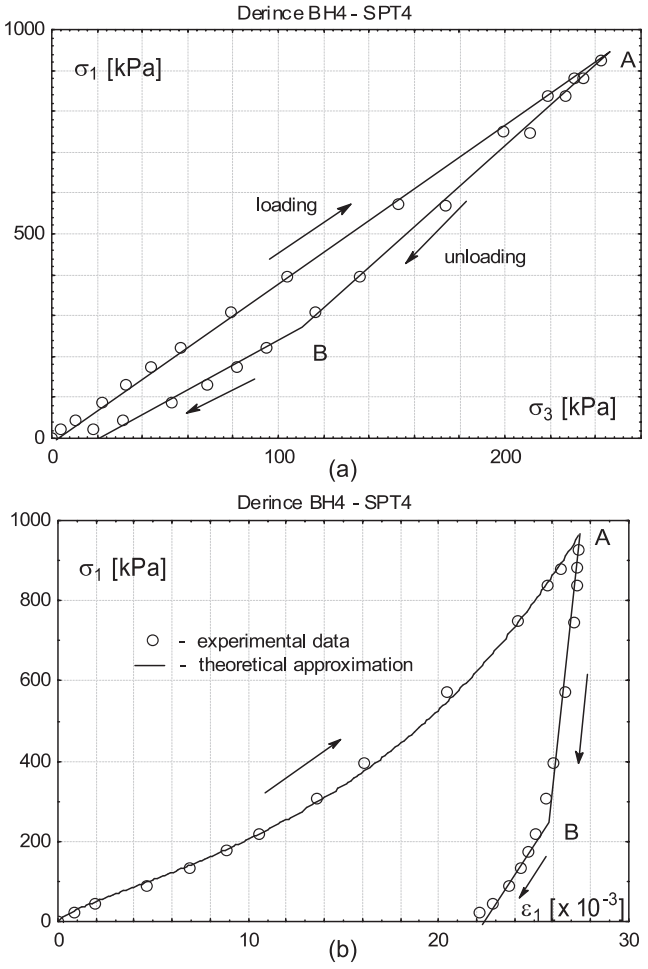

Fig. 12. Piece-wise linear approximation of oedometric unloading for BH4 SPT4 soil sample

The unloading branch of the vertical stress-strain diagram can be approximated by two sectors, as shown in Fig. 12a. Similar, piece-wise linear approximation of the vertical stress σ_1 –

Table 2
Compaction coefficients for soils taken from boreholes BH1-BH5, cf. Fig. 2

Borehole	No. of sample	Soil	$D_r^*[\%]$	C_1	C_2	D_1	D_2
BH1	SPT 2	MS	33.7	6.53	0.154	1.01	0.153
	SPT 2	G-M (S-M)**	34.3	9.50	0.266	2.53	0.105
	SPT 5	SM	48.3	9.00	0.225	2.03	0.111
BH2	SPT 4	S-M	27.73	10.68	0.150	1.60	0.094
	SPT 5	SM	38.53	8.57	0.187	1.60	0.116
	SPT 7	M	39.33	6.76	0.242	1.64	0.148
	SPT 1	S-M+G	42.59	7.88	0.258	2.03	0.127
BH4	SPT 3	SW+G	22.66	10.93	0.141	1.54	0.091
	SPT 4	S-M+G	54.14	9.00	0.219	1.97	0.111
BH5	SPT 3	S-M+G	44.79	9.57	0.348	3.33	0.104
	SPT 5	S-M	76.12	3.66	0.264	0.97	0.273

* – mean value of initial relative density from the series of several tests for each strain amplitude. The density in the tests corresponds to the in-situ density measured by SPT

Table 3
Elastic and mechanical properties of investigated soils

Borehole	No. of sample	D_r^* [%]	E ($\times 10^8$ N/m^2)	ν	κ_s ($\times 10^{-8}$ m^2/N)	K_0	G_1 ($\times 10^8$ N/m^2)	ϕ
BH1	SPT 2	31.8	0.25	0.184	7.58	0.295	0.37	37.96
BH2	SPT 2	34.3	3.02	0.204	0.59	0.320		
	SPT 5	54.1	2.35	0.19	0.79	0.291	0.55	36.25
	SPT 4	33.3	2.44	0.218	0.69	0.36	0.52	32.0
BH3	SPT 5	43.0	2.65	0.205	0.67	0.34	0.51	31.52
	SPT 7	74.3	2.28	0.179	0.84	0.308		34.5
	SPT 1	33.0	2.50	0.203	0.71	0.333	0.77	
BH4	SPT 3	13.6	2.99	0.199	0.60	0.312	0.67	38.6
	SPT 4	83.7	3.32	0.173	0.59	0.28		
BH5	SPT 3	46.7	3.02	0.209	0.58	0.344		
	SPT 5	42.5	2.54	0.209	0.69	0.317	0.88	35.6

* – mean value of initial relative density from the series of at least three tests. The density in the tests corresponds to the in-situ density measured by SPT

horizontal stress σ_3 relation is shown in Fig. 12b. The sectors AB correspond to purely elastic response of the soil. Poisson's ratio can be calculated from the following formula:

$$\nu = \frac{1}{1+m}, \tag{17}$$

where:

$$m = \frac{\sigma_1^A - \sigma_1^B}{\sigma_3^A - \sigma_3^B}, \tag{18}$$

and the Young modulus is given by the following expression:

$$E = E^* \left[1 - \frac{2}{m\,(1+m)}\right], \tag{19}$$

where E^* = slope of the unloading sector AB in the σ_1, ε_1 space, cf. Fig. 12a.

Elastic compressibility of the soil skeleton is therefore:

$$\kappa_s = \frac{3\,(1-2\nu)}{E}. \tag{20}$$

Oedometric tests have also served to determine the coefficient of the earth pressure at rest K_0. Table 3 summarizes the results of experimental tests together with the values of the angle of internal friction of investigated soils. For each soil sample, the series of minimum three tests were carried out. The values given below are the averages obtained from these tests.

9. Prediction of pore-pressure generation and liquefaction

The most important problem in earthquake geotechnics is to predict liquefaction potential of a given site. The first step of practically useful assessment of liquefaction potential is the analysis of some empirical data, as the grain size distribution curves and SPTs results, as discussed in Section 4. The next step of analysis includes more detailed studies of the behaviour of particular sites, based on both empirical and analytical methods. Some suggestions regarding these methods are recommended in recent guidelines, see [12,13]. The most recommended method is the simplified procedure proposed by Seed and Idriss [19], and then perfected by generations of researchers [12]. The current shape of this procedure does not differ essentially from the original, except for a variety of very

detailed changes, dealing with the values of particular coefficients, etc. In this paper, we are not going to examine in detail these achievements and the current state of empirical knowledge about the assessment of liquefaction potential of soils, but we would like to follow this type of methodology.

The basic problem is to assess the earthquake-induced shear stresses at the site. In order to do this, one has to assume a design earthquake, which is certainly not the aim of the geotechnical engineer, but rather seismologists. It is assumed, in this paper, that the design earthquake is known. Therefore, as the first step of our analysis, we have to determine the shear stresses in a given soil stratum for the assumed earthquake. Then, for this input, we have to determine the number of equivalent loading cycles causing liquefaction of particular layers of the soil stratum. Such a procedure is very rough, as it affords only general information as to the behaviour of a saturated soil stratum during the earthquake excitations.

It is probably impossible to work out a precise method which would enable predictions of soil behaviour in seismic areas, as we lack the basic information, including data concerning the design earthquake, detailed properties of particular sites, etc. It is, however, possible to estimate the liquefaction properties of soils, with sufficient accuracy for engineering purposes.

In this paper, we are going to propose a certain alternative to the classic procedures of assessment of liquefaction potential of soils. Classic procedures require laboratory investigations on liquefaction of undrained soil samples, in order to determine the number of equivalent cycles causing liquefaction of specimens subjected to a given confining stress. Instead of these experiments, we propose an analytical estimation of liquefaction potential, based on solving a simple differential equation, which follows the C/L theory. Such a procedure is cheaper than costly experimental investigations, and also has specific advantages, as different cyclic shear stress histories can be analysed fairly easily.

9.1. Estimation of earthquake-induced shear stresses. In order to estimate the earthquake-induced shear stresses in a soil stratum, various procedures can be applied. The most common one was proposed by Seed and Idriss [19], and this procedure is still recommended in recent guidelines [12,14]. The average earthquake-induced cyclic stress ratio (CSR) in a soil stratum is given by the following relation:

$$\frac{\tau_0}{\sigma_v'} = 0.65 \left(\frac{A_{\max}}{g} \right) \left(\frac{\sigma_v}{\sigma_v'} \right) r_d, \tag{21}$$

where: τ_0 = maximum shear stress; σ_v' = effective vertical overburden stress; σ_v = total vertical overburden stress; $A_{\max}$ = peak horizontal acceleration at ground surface; g = acceleration of gravity; r_d = stress reduction coefficient, decreasing with depth.

The coefficient r_d was introduced in Eq. (19) in order to take into account deformability of the soil stratum. Youd et al. [12] suggest extremely precise values of this coefficient, with an accuracy of the order of 10^{-5}. Such accuracy seems rather exaggerated, as geotechnical measurements are usually carried out with an accuracy of the order of 10^{-1}!. The Iwasaki formula, after [14], would seem to be much more practical:

$$r_d = 1 - 0.015z, \tag{22}$$

where z = vertical co-ordinate in meters, see Fig. 13.

The above described procedure has been verified empirically, with various case history data, down to a depth of 15 m, which seems to be most important for geotechnical engineers [12].

Equation (21) served to calculate CSR in interpretation of SPTs results presented in Section 4 of this paper.

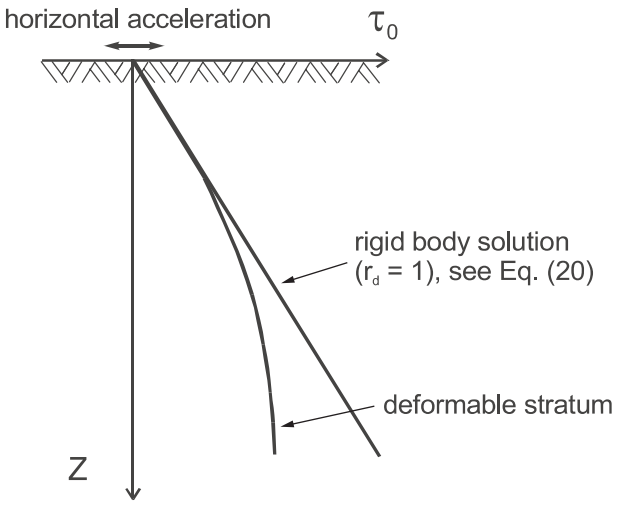

Fig. 13. Maximum shear stresses in soil stratum

Equation (21) has been derived on the basis of some simple considerations regarding the behaviour of a soil stratum subjected to cyclic horizontal acceleration at ground surface level. Simple analysis of equilibrium leads to the following expression for the shear stresses:

$$\tau_0 = A_{\max} \rho z, \tag{23}$$

where ρ = density of the soil. Because $\rho = \gamma/g$, where γ = unit weight of the soil, Eq. (21) can be obtained easily. Note that the shear stress given by Eq. (23) does not depend on mechanical properties of the soil (mainly on the shear modulus), hence the stress reduction coefficients were introduced: r_d for the soil "flexibility" and 0.65 for the average stress.

Such a method of estimation of earthquake-induced shear stresses, although commonly accepted as geotechnical standard, provokes many questions from the point of view of applied mechanics. It should be noted first, that earthquake-induced shear stresses have never been measured in real field conditions. Therefore, direct comparisons of procedures proposed with real case history data is impossible. It is possible, however, to find more realistic estimates of shear stresses than Eq. (23), using well known methods of mechanics.

For example, for the sinusoidal cyclic horizontal acceleration at ground surface level:

$$A = A_0 \sin \omega t, \tag{24}$$

where ω = frequency of shaking, the governing equations for the problem of determination of shear stresses are the following, (see Fig. 13):

$$\frac{d^2\tau_0}{dz^2} + \frac{\rho\omega^2}{G}\tau_0 = 0, \tag{25}$$

$$\left.\frac{d\tau_0}{dz}\right|_{z=0} = \rho A_0, \ \tau_0\,(z=0) = 0. \tag{26}$$

The solution of the boundary-value problem, defined by Eqs. (25) and (26), depends on the shape of function describing the shear modulus G.

In the most simple case of G = const, the solution of Eqs. (25) and (26) is the following:

$$\tau_0 = \frac{\rho A_0}{k}\sin kz, \quad k = \sqrt{\frac{\rho\omega^2}{G}}. \tag{27}$$

For small values of kz, there is $\sin kz \approx kz$, and in this case Eq. (27) reduces to Eq. (23).

In a more realistic case, where $G = G(z)$, the analytical solution of Eqs. (25) and (26) is more difficult to obtain. If we assume $G = G_0 z$, Eq. (25) can be rewritten in the form of a Bessel type differential equation, the solution of which is built of Bessel functions. This solution can also be expressed as the following infinite series:

$$\tau_0 \cong \rho A_0 \left[z - \frac{k^2 z^2}{2} + ...\right], \tag{28}$$

where $k^2 = \rho\omega^2/G_0$.

Note that for small values of kz, the second and higher order terms can be neglected in Eq. (28), which again reduces to Eq. (23). If we retain only the first terms of Eq. (28), and neglect the other, the second term will give the stress reduction. This stress reduction does not depend solely on z, like the stress reduction factor r_d, but also depends on ω and G_0!

Similar procedure can be applied for $G = G_0\sqrt{z}$. Again, Eq. (25) can be re-written as a Bessel type differential equation, etc. Some exact solutions of this problem, but for slightly different boundary conditions, are presented in [20], see also [21].

The above discussion shows that Eq. (23) may really serve as a reasonable estimate of the shear stresses induced by earthquake. This estimate has a meaning of the first term of infinite series representing the more exact solution of the problem considered. However, the averaging factor 0.65 in Eq. (21) has no rational meaning if we consider sinusoidal acceleration, as the average shear stress $\tau_0 = \tau_{\max}$ in this case, and there is no necessity to reduce this value.

What is most important, in the case of pore-pressure generation and liquefaction of a soil stratum, is that the shear modulus $G = G(p')$, cf. Eq. (16). During the process of pore-pressure generation, the mean effective stress p' decreases, hence the shear modulus also decreases, which is not reflected in the simplified procedure. In order to take this phenomenon into account, Eq. (25) with $G = G(p')$, should be solved for given site conditions. In such a case we have to know the equation describing the pore-pressure generation, which does not appear in the simplified procedure. Sawicki [10] and Sawicki and Świdziński [11] show how this can be done.

9.2. Equivalent number of loading cycles. According to the simplified procedure, one has to compare the cyclic stress ratio, given by Eq. (21), with the cyclic stress ratio inducing liquefaction at a given number of loading cycles, which has been designated as the "equivalent number of cycles". The equivalent number of cycles, at given average shear stress amplitude, has been related to the magnitude of design earthquake, after some statistical analyses. For example, for the earthquake of the magnitude 7.5 (roughly the Kocaeli earthquake), the number of significant stress cycles is 20, according to [19]. More recent guidelines suggest some reduction of this number, to 15, cf. Foray (2002).

Very detailed prescriptions of how to calculate a number of equivalent loading cycles is also presented in the textbook of Das [21], after the works of Seed and his co-workers. He shows how to determine the equivalent number of uniform stress cycles of the amplitude $0.65\tau_{\max}$, on the basis of known irregular stress-time history, where $\tau_{\max}$ = maximum shear stress. Such a procedure also provokes many doubts from the analytical point of view.

Firstly, it is hard to evaluate a design seismic load, mainly the history of horizontal cyclic acceleration on the ground surface at specific sites. It follows from historical records that such histories can be represented as random time series, with also random location of the peak accelerations. Such a type of loading strongly influences the behaviour of particular soil sites, as the saturated soils react in a non-linear way, which means that the history of loading significantly influences the behaviour of such sites. For example, consider two simplified histories of the cyclic shear stresses at the given soil element, shown in Fig. 14. These stress histories are characterized by the same mean cyclic stress amplitude $\tau_0/2$.

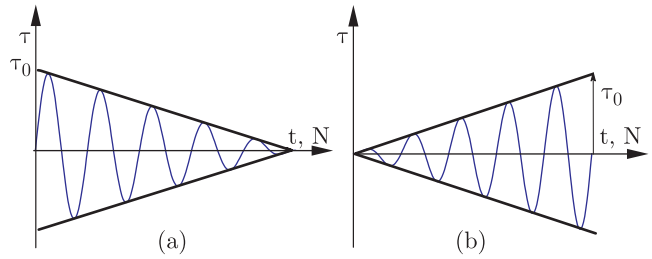

Fig. 14. Different cyclic loading stress histories characterized by the same mean cyclic stress amplitude

The envelope of cyclic stress amplitudes, in the case shown in Fig. 14a, is the following:

$$\tau = \pm\tau_0\left(1 - \frac{N}{5}\right), \tag{29}$$

and in the case from Fig. 14b:

$$\tau = \pm\tau_0\frac{N}{5}. \tag{30}$$

In both cases, the period T of cyclic loading is constant. Application of the procedure described in Das [21], Section 8.8

in the second edition of this textbook, gives the average number of equivalent loading cycles, at $0.65\tau_{\max} = 0.65\tau_0$, $N = 4$. According to Das, the term "equivalent" means that the effect of any irregular stress-time history should be the same as the effect caused by uniform equivalent stress cycles. In the case considered, it means that 4 cycles of constant stress amplitude $0.65\tau_0$ should give the same effect as the effects caused by the cyclic stress histories shown in Fig. 14. Such a procedure is controversial from the analytical point of view, as the behaviour of saturated soils is history dependent, and therefore the sequence of loading cycles is of basic importance. It will be shown in the next Section, that the cyclic stress histories shown in Fig. 14 give very different pore-pressure accumulation histories, with the onsets of liquefaction also differing.

9.3. Pore-pressure generation and onset of liquefaction. It is suggested, in the simplified procedure, that cyclic loading laboratory investigations be conducted on saturated soil samples in order to determine shear stresses causing liquefaction, for various confining pressures, and for the number of equivalent cycles. These stresses should be then compared with those estimated in the field in order to determine liquefaction zones in the soil stratum.

An alternative method is to predict the process of pore-pressure generation and onset of liquefaction, using the C/L model described in Section 5, for the soil parameters presented in Sections 6–8. In the case of simple cyclic shearing of a saturated soil sample in undrained conditions, Eqs. (3)-(8) and (10) lead to the following differential equation for the pore-pressure generation:

$$\frac{du}{dN} = \frac{D_1\tau^2}{4aG_1^2}\frac{1}{\left(p_0' - u\right)}\exp\left(-D_2 a u\right), \qquad (31)$$

where: u = excess pore pressure generated by cyclic loading; p_0' = initial mean effective stress. The initial condition is obviously $u(N=0) = 0$.

Recall that Eq. (31) describes the pore-pressure generation in a single soil element. This equation is an analytical equivalent of experimental simple cyclic shearing of soil in undrained conditions, for the given history of cyclic loading $\tau = \tau(N)$. The simplest method of solving Eq. (31) is by numerical integration.

9.4. Examples. Consider first the uniform cyclic loading, at constant shear stress amplitude $\tau = \tau_0 = 0.15$ (in stress unit 10^5 N/m^2) of the saturated soil sample, subjected to the initial confining effective stress $p_0' = 0.5$ (in stress unit 10^5 N/m^2). The other data, corresponding to the Derince sand, are the following $D_1 = 1.97$; $D_2 = 0.14$; $a = 1.044$ (in compressibility unit 10^{-8} m^2/N); $G_1 = 0.77$. The excess pore-pressure *u* generated by cyclic loading, is expressed also in stress unit 10^5 N/m^2. The above numbers were substituted in Eq. (31) and this equation then being numerically integrated.

Figure 15 illustrates the excess pore-pressure generation in the sample. Liquefaction corresponds to $N = 7.3$, as $u = 0.5 = p_0'$, which means that the effective mean stress $p' = p_0' - u = 0$ at $N = 7.3$ cycles.

Figure 16 illustrates the corresponding increase of the cyclic shear strain amplitude γ_0 (expressed in strain unit 10^{-3}). The strain amplitude slowly increases up to approximately $N = 6$ loading cycles, this increase then becoming more rapid. This is a consequence of subsequent reduction of the mean effective stress due to the pore-pressure accumulation, and resulting reduction of the shearing resistance of saturated soil sample. At the onset of liquefaction ($N = 7.3$), the shear strain rapidly increases.

The other interesting example deals with the behaviour of similar soil samples subjected to different cyclic stress histories, shown in Fig. 14. According to the simplified procedure, both stress histories should give the same result as they can be replaced by 4 uniform cycles of the amplitude of $0.65\tau_0$.

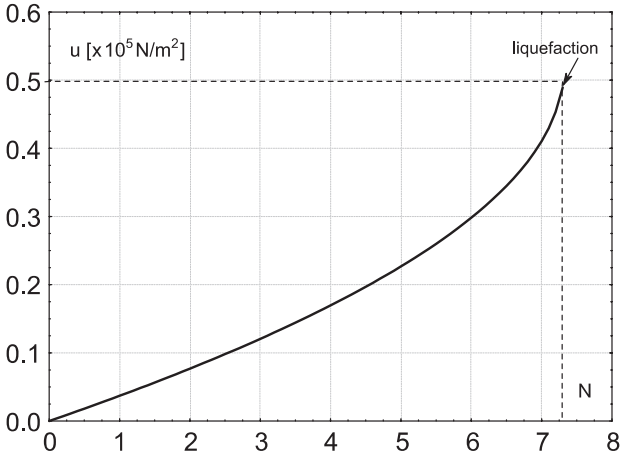

Fig. 15. Pore-pressure generation in the Derince soil sample subjected to uniform cyclic shearing, at constant shear stress amplitude $\tau_0 = 0.15 \times 10^5$ N/m^2

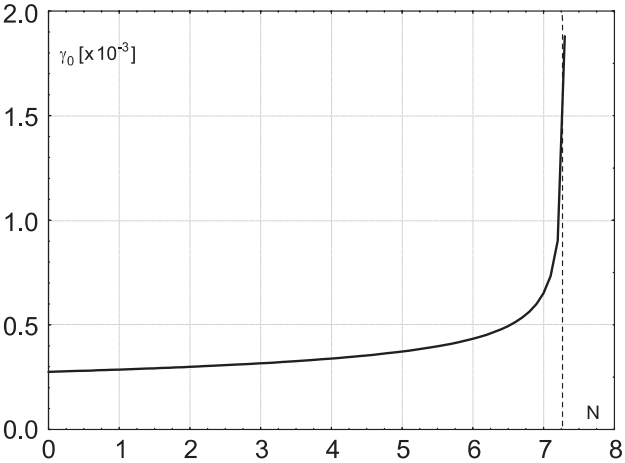

Fig. 16. Development of cyclic shear strain amplitude corresponding to the pore-pressure generation shown in Fig. 15

Figure 17 shows the histories of pore-pressure generation and the onset of liquefaction for the Derince soil (data as in the previous example) subjected to the stress histories, shown in Figure 14, and to 4 equivalent loading cycles. The other data are the following: $\tau_0 = 0.5$ and $p_0' = 0.5$ and 0.7, all in unit 10^5 N/m^2.

In both cases presented, three different histories of the pore-pressure generation were obtained. The cyclic shear stress history shown in Fig. 14a gives the most rapid increase of excess pore-pressure and the onset of liquefaction. In the case of $p'_0 = 0.5$, liquefaction takes place in the first loading cycle ($N = 0.75$), whilst the stress history shown in Fig. 14b produces liquefaction in the 4^{th} cycle ($N = 3.7$). Equivalent uniform stress cycles of the amplitude of $\tau = 0.65\tau_0 = 0.325$ produce liquefaction within the 2nd cycle ($N = 1.5$). Results shown in Fig. 17b correspond to a higher value of the initial mean effective stress $p'_0 = 0.7$. Qualitatively, the character of pore-pressure generation is similar to that shown in Fig. 17a., but the liquefaction is produced later, obviously because the initial mean effective stress is bigger.

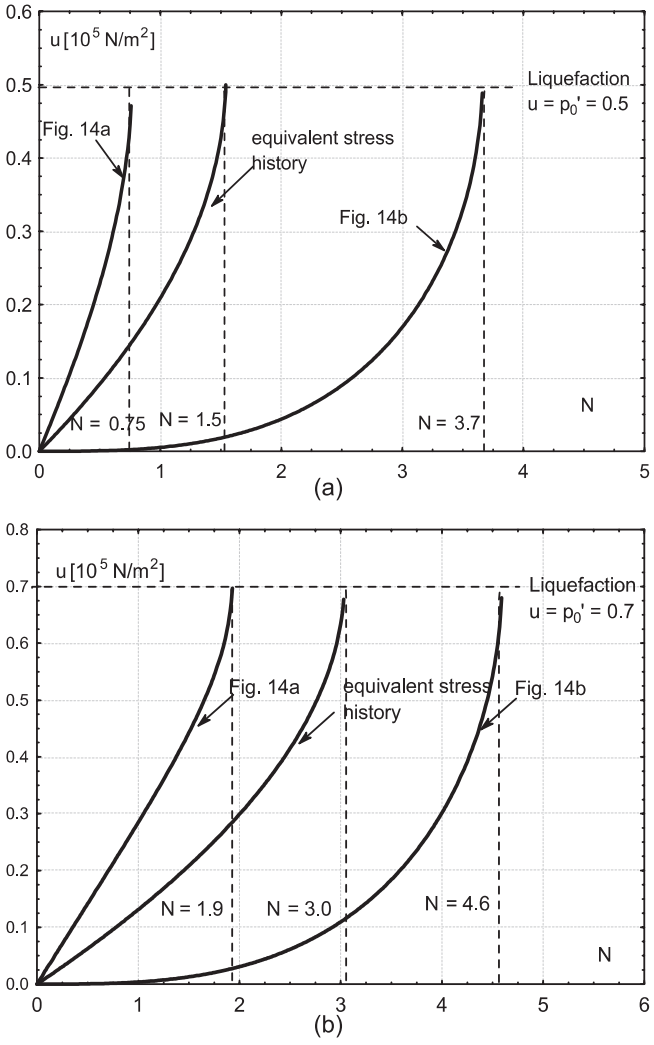

Fig. 17. Histories of pore-pressure generation and onset of liquefaction in Derince soil (a) $\tau_0 = 0.5$, $p'_0 = 0.5$; (b) $p'_0 = 0.7$

Similar results have been obtained for the Eregli soil ($D_1 = 1.60$, $D_2 = 0.105$, $a = 0.694$, $G_1 = 0.52$). Fig. 18 illustrates some histories of the pore-pressure generation and liquefaction.

In the case of $p'_0 = 1$ (in unit 10^5 N/m^2), the behaviour of Eregli soil (see Fig. 18a) is qualitatively similar to that of Derince soil, shown in Fig. 17. However, the histories of pore-pressure generation shown in Fig. 18b differ slightly from the qualitative point of view. These histories correspond to $p'_0 = 1.5$, and none of them leads to liquefaction. The stress histories from Fig. 14 are qualitatively different, but accidentally produce the same excess pore-pressure after 5 cycles of loading.

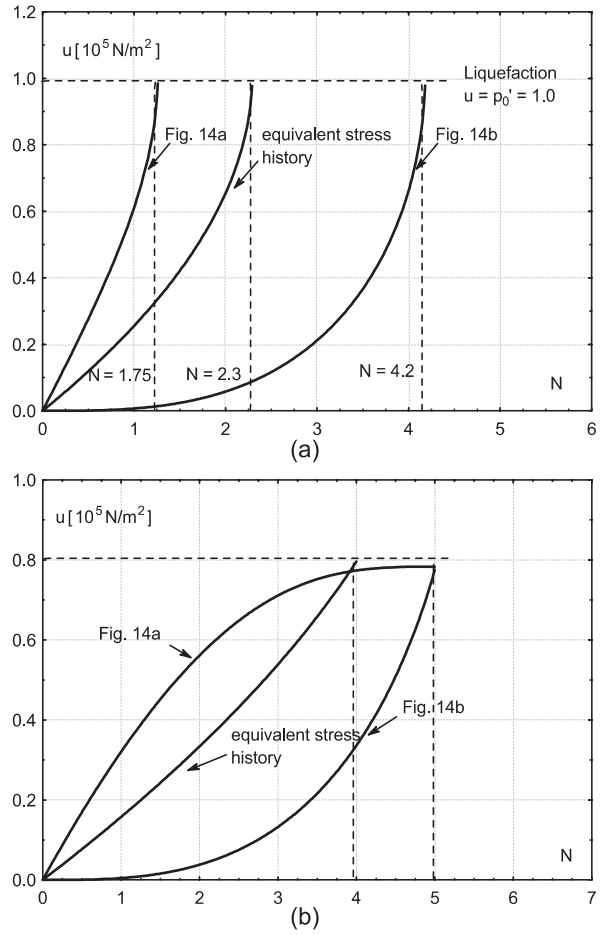

Fig. 18. Histories of pore-pressure generation and onset of liquefaction in Eregli soil, (a) $p'_0 = 1$; (b) $p'_0 = 1.5$

Recall that the histories of pore-pressure generation, shown in Figs. 15, 17 and 18, were obtained from integration of Eq. (31). The solution of this equation depends on the following four parameters: D_1, D_2, a and G, which characterize the compaction/liquefaction properties of a given soil. It also depends on the initial mean effective stress p'_0, and the history of cyclic loading $\tau = \tau(N)$.

It should be added that constants D_1 and D_2 depend on the initial relative density D_r of a soil sample. Therefore, the histories of pore-pressure generation also depend on D_r.

9.5. Discussion. The behaviour of actual saturated soils is highly complex, and there does not exist a general theory that describes all the features of this complex behaviour. However, there exist some formally simple theories which describe only some chosen features of the behaviour of granular media, neglecting the effects which are not important from the point of view of a particular problem. The most pronounced example

of such a partial theory is the model of limit states, which is very well elaborated in soil mechanics, and is also useful from the practical point of view. Even the theory of elasticity has found very wide applications in soil mechanics, although actual soils are certainly not the elastic materials. In this context, we have to analyse the existing approaches to the problem of pore-pressure generation in granular soils subjected to cyclic loadings.

The "Simplified Procedure" is based on extensive empirical investigations, but it has not the status of a theory, although it can form some background for practically useful models (theories). The C/L model has the status of an engineering theory, formulated within the framework of applied mechanics. This model is fairly simple from the point of view of applications, but this simplicity has been achieved at the expense of some approximations. One of the basic approximations deals with the resolution of the stress and strain tensors on the "static" and "cyclic" parts. Such a resolution enables simple formulation of the C/L theory, but at the cost of preciseness. The C/L model can be classified as a "low resolution" one, as it displays only some basic features of the compaction and liquefaction related phenomena, but may sometimes violate other principles of soil mechanics. For example, the Coulomb-Mohr failure criterion may be exceeded at the onset of liquefaction, defined by the C/L theory. Therefore, the C/L theory gives only some approximated picture of the behaviour of saturated soils subjected to cyclic loadings, similar to the classical models of structural mechanics and strength of materials. It should also be mentioned that the "Simplified Procedure" has similar shortcomings.

10. Discussion and conclusions

In the present paper, a systematic analysis of liquefaction susceptibility of some soils from the coast of the Marmara Sea is presented. The investigations presented include:

- Field investigations;
- Laboratory determination of physical and mechanical properties of soils;
- Preliminary analysis of liquefaction susceptibility using standard geotechnical methods
- Analytical studies of the process of pore-pressure generation and onset of liquefaction.

The main results presented in this paper are the following:

- Determination of physical and mechanical properties of some chosen soils from sites where liquefaction had occurred during the Kocaeli earthquake. The presented data, obtained from extensive laboratory and field investigations, being unique, should be useful for other researchers, in earthquake geotechnics.
- Presentation of a systematic approach to the analysis of liquefaction susceptibility of soils in seismic areas, being based on the compaction/liquefaction model. A unique result is that the parameters of this model have been determined experimentally for given Turkish soils. The model presented may supplement already existing guidelines. The approach proposed does not require laboratory investigations of liquefaction of saturated soil samples, but only integration of a simple differential equation describing pore-pressure generation and onset of liquefaction for a given cyclic shear stress history.
- Discussion of standard geotechnical procedures, from the analytical point of view, may be useful in further refinement of these procedures. This discussion also displays some links between purely empirical and analytical approaches to the problem of estimation of liquefaction susceptibility of saturated soils.

The main conclusions which follow from this paper are:

- The first step of empirical assessment of liquefaction susceptibility, based on the analysis of the grain size distribution curves, shows that generally the investigated soils are susceptible to liquefaction. It should be noted, however, that the shape of the grain size distribution curves provides only very rough information as to the liquefaction potential, because many other important factors, such as the initial relative density, cyclic loading history, etc., are not taken into account.
- The analysis of SPTs does not provide unique information as to the liquefaction potential of the sites investigated. Note that these tests were performed on sites after liquefaction had taken place. Interpretation of SPTs for Turkish soils differs from that obtained from the analysis of grain size distribution curves and in some cases is inconsistent with post-earthquake observations with regard to liquefaction susceptibility of investigated soils.
- Analytical procedure, based on the C/L theory, offers realistic predictions as to the liquefaction potential of the sites investigated, at least from the qualitative point of view. It was shown that the soils investigated would liquefy when subjected to cyclic loading histories that probably had occurred during the Kocaeli earthquake. The analysis presented in this paper supplements other analyses, based on solving initial/boundary value problems for the sites investigated, already presented in [10,11].
- It is believed that the systematic approach to the problem of assessment of liquefaction potential of saturated soils, presented in this paper, would supplement already existing methods.

Acknowledgements. This study has been performed within the European Commission Research Directorates' FP5, the LIMAS-Project (Liquefaction Around Marine Structures, Contract No.EVK3-CT-2000-00038). ECRD financial support for IBW PAN is gratefully acknowledged. The authors would like to thank Professor B. M. Sumer, Project Co-ordinator, as well as the Steering Committee and all the partners involved, for enabling IBW PAN participation in LIMAS.

REFERENCES

[1] A.S. Cakmak, "Soil dynamics and liquefaction", *Developments in Geotechnical Engineering* 42, 378 (1987).

[2] K. Ishihara, *Soil Behaviour in Earthquake Geotechnics*, Oxford: Clarendon Press, 1996.
[3] P.V. Lade and J.A. Yamamura, *Physics and Mechanics of Soil Liquefaction*, Balkema, Rotterdam, 1999.
[4] R.Y.S. Pak, and J. Yamamura, *Soil Dynamics and Liquefaction*, Geotechnical Special Publication, ASCE and GeoInstitute, Denver, 2000.
[5] A. Sawicki and J. Mierczyński, "Development in modelling liquefaction of granular soils caused by cyclic loads", *Applied Mechanics Reviews*, 59, 91–106 (2006).
[6] T.L. Youd, J.P. Bardet, and J.D. Bray, "Earthquake of August 17, 1999 Kocaelli. Reconnaisance report", *Earthquake* 16, (2000).
[7] B.M. Sumer, A. Kaya, and N.E. Ottesen Hansen, "Impact of liquefaction on coastal structures in the 1999 Kocaeli, Turkey earthquake", *Proc. 12th Int. Offshore and Polar Eng. Conf*: II, 504–511 (2002).
[8] Y. Yuksel, B. Alpar, A.C. Yalciner, E. Cevik, O. Ozguven, and Y. Celikoglu, "Effects of the Eastern Marmara earthquake on the marine structures and coastal areas", *Proc. Institution of Civil Engineers. Water and Maritime Engineering* 154, 1–17 (2003).
[9] A. Sawicki, "An engineering model for compaction of sand under cyclic loading", *Engineering Transactions* 35(4), 677–693 (1987).
[10] A. Sawicki, "Modelling earthquake-induced phenomena in the Izmit Bay coastal area", *Cyclic Behaviour of Soils and Liquefaction Phenomena*, Balhema 431–440 (2004).
[11] A. Sawicki and W. Świdziński, "Liquefaction and settlements of backfill behind quay-walls caused by seismic loads", *Cyclic Behaviour of Soils and Liquefaction Phenomena*, Balhema 441–448 (2004).
[12] T.L. Youd, M.L. Idriss, R.D. Andrus, I. Argano, G. Castro, J.T. Christian, R. Dobry, W.D.L. Finn, L.F. Harder, M.E. Hynes, K. Ishihara, J.P. Koester, S.S.C. Liao, F.W. Marcuson, G.R. Martin, J.K. Mitchell, Y. Moriwaki, M.S. Power, P.K. Robertson, R.B. Seed, and K.H. Stokoe, "Liquefaction resistance of soils: summary report from the 1996 NCEER and 1998 NCEER/NSF workshops on evaluation of liquefaction resistance of soils", *J. Geotech. Eng. ASCE* 127 (10), 817–833 (2001).
[13] PIANC 2001, *Seismic Design Guidelines for Port Structures*, Balkema, Lisse/Abingdon, 2001.
[14] P. Foray, "Liquefaction of soils", *Proc. of B.E.S.T. School on Natural Hazards and Infrastructures*, Grenoble, 2002.
[15] S. Liao, and R.V. Whitman, "Overburden correction factors for SPT in sand", *J. Geotech. Eng. ASCE* 112 (3), 373–377 (1986).
[16] A. Sawicki, and W. Świdziński, "Mechanics of a sandy subsoil subjected to cyclic loadings", *Int. J. Numerical Analytical Methods in Geomechanics* 13, 511–529 (1989).
[17] A. Sawicki, "Elasto-plastic interpretation of oedometric test", *Arch. Hydro-Engineering and Environ. Mech.* 41 (1–2), 111–131 (1994).
[18] A. Sawicki and W. Świdziński, "Elastic moduli of non-cohesive particulate materials", *Powder Technology* 96, 24–32 (1998).
[19] H.B. Seed and I.M. Idriss, "Simplified procedure for evaluating soil liquefaction potential", *J. Soil Mechanics and Foundations Division, ASCE* 97 (SM9), 1249–1273 (1971).
[20] J. Przewłócki and W. Knabe, "Settlement of a soil stratum subjected to an earthquake", *Int. J. Numerical Analytical Methods in Geomechanics* 19, 813–821 (1995).
[21] B.M. Das, *Fundamentals of Soil Dynamics*, Elsevier, Oxford, 1983.